

See discussions, stats, and author profiles for this publication at: <https://www.researchgate.net/publication/204978640>

In-Line Esterification of Pyrolysis Vapor with Ethanol Improves Bio-oil Quality

ARTICLE *in* ENERGY & FUELS · JANUARY 2010

Impact Factor: 2.79 · DOI: 10.1021/ef900838g

CITATIONS

39

READS

60

4 AUTHORS, INCLUDING:



[Roger Norris Hilten](#)

University of Georgia

22 PUBLICATIONS 263 CITATIONS

SEE PROFILE



[James Robert Kastner](#)

University of Georgia

63 PUBLICATIONS 825 CITATIONS

SEE PROFILE



[K.C. Das](#)

University of Georgia

131 PUBLICATIONS 3,424 CITATIONS

SEE PROFILE

In-Line Esterification of Pyrolysis Vapor with Ethanol Improves Bio-oil Quality

Roger N. Hilten,* Brian P. Bibens, James R. Kastner, and K. C. Das

Driftmier Engineering Center, The University of Georgia, Athens, Georgia 30602

Received July 31, 2009. Revised Manuscript Received October 7, 2009

A simple reactive condensation technique was developed to decrease the concentration of reactive species in the oily phase of two-phase pyrolysis oil as a means to increase the storage stability, heating value, and overall quality of the oil. Bio-oil vapor was esterified from the reaction of in situ organic acids with ethanol during condensation resulting in the production of water and esters. The research compared the quality of slow pyrolysis-produced bio-oils collected by condensing pyrolysis vapor using atomized ethanol (EtOH) at various weight hourly space velocity (WHSV). The resultant bio-oil exhibited two phases at room temperature, which were separated to obtain an oily and an aqueous phase. WHSV was varied from 8.3 to 33 (kg h^{-1} biomass per kg h^{-1} ethanol), which produced bio-oils with ethanol content ranging from 7.3 to 23.2 wt % of total oil. Increasing EtOH from 0 to 23% (w/w) decreased water content and viscosity in the oily phase by 16% and 56%, respectively, while also increasing pH from 2.48 to 3.05. Results were consistent with the formation of esters. The concentration of a carboxylic acid, acetic acid, and an ester, ethyl acetate, were determined using quantitative GC-MS analysis and indicated a maximum 40% (v/v) conversion of acetic acid with 19% (v/v) being converted to ethyl acetate. Other reactions predicted included acetalizations of formaldehyde and acetaldehyde with ethanol to form diethoxymethane and 1,1-diethoxyethane, respectively.

Introduction

Pyrolysis oil, or bio-oil, is a potential source of renewable energy for electricity, heat generation, and as a transportation fuel. However, several obstacles must be overcome before bio-oil can be used reliably as a fuel. One of the main issues is poor storage stability of the oils. During storage, there is potential for bio-oils to undergo changes because of oxidative and thermal degradation. Oxidation can lead to polymerization resulting in viscosity increases. Thermal degradation causes partial decomposition of components and can lead to loss of volatiles. Storage in both oxidative and elevated temperature conditions lead to physical changes (e.g., viscosity increases and heating value decreases) and compositional changes.^{1–4} Most applications for bio-oils require that bio-oils retain favorable initial physical properties during storage, shipment, and use.³ Otherwise, filters, injectors, input lines, etc. may become obstructed. In addition, the high level of reactive species and water content of bio-oil makes it unstable under normal storage conditions, which lead to increased viscosity over time. In addition, high oxygen and water content also lower the heating value of the fuel.⁴

During aging, bio-oil viscosity and chemical composition change dramatically mainly because of polymerization reactions.⁵ A higher degree of polymerization results in an increase in viscosity. Polymerization reactions that lead to viscosity increases are accelerated at higher storage temperatures where it has been shown that viscosity can increase from $0.009 \text{ cP day}^{-1}$ when stored at -20°C to more than 300 cP day^{-1} at 90°C .⁵ However, it has been shown that adding solvents after pyrolysis can increase the stability of bio-oil during aging. Diebold and Czernik² showed that additions of solvents could significantly decrease viscosity changes during aging. Solvents used in the study included ethyl acetate, a mixture of methyl isobutyl ketone and methanol, acetone, methanol, a mixture of acetone and methanol, and ethanol. Their findings revealed that 10% (w/w) methanol enhanced bio-oil stability most effectively.

The immediate effects of adding an alcohol are decreased viscosity and increased heating value.^{6–8} These improvements to bio-oil make it more favorable for combustion applications, such as in furnaces, boilers, and gas turbines, or as an alternative to diesel where untreated bio-oils can require major changes to existing systems.^{8,9} The increase in heating

*To whom correspondence should be addressed. Phone: +1 706 542 6681. Fax: +1 706 542 8806. E-mail: rhilten@engr.uga.edu.

(1) Boucher, M.; Chaala, A.; Pakdel, H.; Roy, C. Bio-oils obtained by vacuum pyrolysis of softwood bark as a liquid fuel for gas turbines. Part II: Stability and ageing of bio-oil and its blends with methanol and a pyrolytic aqueous phase. *Biomass Bioenergy* **2000**, *19*, 351–361.

(2) Diebold, J. P.; Czernik, S. Additives to lower and stabilize the viscosity of pyrolysis oils during storage. *Energy Fuels* **1997**, *11*, 1081–1091.

(3) Diebold, J. P. A Review of the chemical and physical mechanisms of the storage stability of fast pyrolysis bio-oils; Subcontractor Report for the National Renewable Energy Laboratory NREL/SR-570-27613; National Renewable Energy Laboratory: Golden, CO, 2000.

(4) Oasmaa, A.; Kuoppala, E. Fast pyrolysis of forestry residue. 3. Storage stability of liquid fuel. *Energy Fuels* **2003**, *17* (3), 1075–1084.

(5) Adjaye, D.; Sharma, R. K.; Bakhshi, N. N. Characterization and stability analysis of wood-derived bio-oil. *Fuel Process. Technol.* **1992**, *31* (3), 241–256.

(6) Moens, L.; Black, S.; Myers, M.; Czernik, S. Study of the neutralization and stabilization of a mixed hardwood bio-oil. *Energy Fuels* **2009**, *23*, 2695–2699.

(7) Oasmaa, A.; Kuoppala, E.; Selin, J.; Gust, S.; Solantausta, Y. Fast pyrolysis of forestry residue and pine. 4. Improvement of the product quality by solvent addition. *Energy Fuels* **2004**, *18*, 1578–1583.

(8) Stamatov, V.; Honnery, D.; Soria, J. Combustion properties of slow pyrolysis bio-oil produced from indigenous Australian species. *Renewable Energy* **2006**, *31*, 2108–2121.

(9) Gust, S. Combustion experiences of flash pyrolysis fuel in intermediate size boiler. In *Developments in Thermal Biomass Conversion*; Bridgewater A. V., Boocock D. G. B., Eds.; Blackie Academic and Professional: London, 1997; pp 481–488.

value for bio-oils mixed with ethanol is because ethanol has a higher heating value of 27 MJ kg⁻¹, which is higher than that of most bio-oils.

Most studies have directly added alcohols after pyrolysis,^{2,6,7} which works well to increase stability and heating value. However, several recent studies^{10–14} showed that using reactive distillation of bio-oil, coupled with an alcohol and an acid or base catalyst, resulted in bio-oil esterification. Esterifying bio-oil can significantly improve the quality of bio-oil by lowering water content, viscosity, and the free-acid content. Additional improvements in bio-oil quality include an increase in heating value by as much as 50%^{10,14} and an increase in stability because of the removal of acids that catalyze polymerization reactions. Junming et al.¹⁰ showed that after three months of aging, esterified bio-oil exhibited very little viscosity increase. Ji-lu¹⁵ introduced well-sprayed ethanol into a bio-oil condenser as a precursor to spraying bio-oil once enough was produced. The intent was to quickly cool vapors to prevent polymerization reactions, though esterification was not observed.

Fischer esterification is proposed to be the reaction pathway in conversion to esters. The esterification reaction follows the equation, $\text{RCOOH} + \text{C}_n\text{H}_{2n+1}\text{OH} \leftrightarrow \text{RCOOC}_n\text{H}_{2n+1} + \text{H}_2\text{O}$, leading to the formation of water and an ester. The simplest ester that can be produced is methyl formate, HCOOCH_3 , when methanol (CH_3OH) is used as the alcohol and is reacted with formic acid, HCOOH . Industrially the reaction is always catalyzed by a strong acid. Several studies^{10,13} have used solid acid catalysts to enhance the bio-oil esterification reaction which improved bio-oil quality by increasing HHV and pH and reducing specific gravity, viscosity and water content for esterified bio-oil.

Several studies^{16–19} have shown the potential to use heterogeneous catalysts for esterifying model bio-oil compounds, such as acetic acid. As an example, Miao and Shanks¹⁹ esterified acetic acid, a model bio-oil compound, using a mesoporous catalyst. Acetic acid conversion was close to 40% at a 250 min reaction time at 50 °C using the catalyst.

Zhang et al.¹⁴ esterified acetic acid in a reflux reactor and showed yields ranging from 15% (no catalyst) to 100% (solid acid catalyst). Koster et al.¹⁸ and Chu et al.¹⁶ performed vapor-phase esterifications of acetic acid with ethanol. Koster et al.¹⁸ performed gas-phase esterifications over several mesoporous catalysts, and showed moderate ester yields (<25%). Equilibrium for the reaction lies far to the right, especially in the vapor phase, for which the thermodynamic equilibrium constant is 367 for the reaction of ethanol and acetic acid to form ethyl acetate.³

In the current study, ethanol was atomized into a stream of uncondensed bio-oil vapor to rapidly and simultaneously cool, condense, and esterify carboxylic acids in the vapor phase. The intent was to increase the quality of bio-oil by effectively removing the undesired acidic compounds. In addition, it is proposed that adding an alcohol during condensation will better stabilize the bio-oil by quickly quenching bio-oil vapor to prevent secondary reactions and by simple dilution of reactive species before reactions can occur. In addition, we theorized that carboxylic acids, likely acetic acid which occurs in high concentration in bio-oil vapor,^{20,21} would undergo Fischer esterification upon mixing with ethanol at elevated temperature to produce esters and water. Water formation should be evident in the overall water balance of pyrolysis. Because of the lower polarity of esters compared to carboxylic acids, the solubility of water in the oily phase of the bio-oil will be reduced. Thus, we expect that water produced during esterification will be concentrated in the aqueous phase of the bio-oil thereby reducing the water content of the oily phase. We also propose that acetalization is occurring following the general equation: $\text{RCOH} + \text{C}_2\text{H}_5\text{OH} \leftrightarrow \text{RCH}(\text{C}_2\text{H}_5)\text{O} - \text{C}_2\text{H}_5\text{O} + \text{H}_2\text{O}$. Additionally, rapid condensation, esterification and acetalization will act to stabilize the bio-oil more effectively than simple condensation thereby increasing thermal and oxidative stability.

Since the reaction equilibrium constant in liquid phase is 4²² compared to 367 in vapor phase,³ we have made the assumption that once bio-oil leaves the heated reaction zone and condenses, esterification essentially ceases. Without a strong acid catalyst, Moens et al.⁶ showed very little reduction in acid number and carbonyl content for bio-oil/methanol mixtures even under heating and proposed that high water content prevents the esterification reaction from going to completion. Though esterification reactions have been proposed to proceed at room temperature without a catalyst,² no quantification has been attempted. The eventual goal is to power a diesel engine with bio-oil that has been upgraded via esterification alone or in combination with other upgrading techniques to improve quality.

Experimental Section

Feedstock. The biomass feedstock used for all experiments was pine wood in the form of pellets supplied by the Southern Shaving Co. located in Cherryville, North Carolina. Pine pellets

(10) Junming, X.; Jianchun, J.; Yunjuan, S.; Yanju, L. Bio-oil upgrading by means of ethyl ester production in reactive distillation to remove water and to improve storage and fuel characteristics. *Biomass Bioenergy* **2008**, 32 (11), 1056–1061.

(11) Lu, C. B.; Yao, J. Z.; Lin, W. G.; Song, W. L. Study on biomass catalytic pyrolysis for the production of bio-gasoline by on-line FTIR. *Chin. Chem. Lett.* **2007**, 18, 445–447.

(12) Mahfud, F.; Melián-Cabrera, I.; Manurung, R.; Heeres, H. Biomass to fuels: Upgrading of flash pyrolysis oil by reactive distillation using a high boiling alcohol and acid catalysts. *Process Saf. Environ. Prot.* **2007**, 85 (5), 466–472.

(13) Tang, Y.; Yu, W.; Mo, L.; Lou, H.; Zheng, X. One-step hydrogenation-esterification of aldehyde and acid to ester over bifunctional Pt catalysts: A model reaction as novel route for catalytic upgrading of fast pyrolysis bio-oil. *Energy Fuels* **2008**, 22 (5), 3484–3488.

(14) Zhang, Q.; Chang, J.; Wang, T.; Xu, Y. Upgrading Bio-oil over Different Solid Catalysts. *Energy Fuels* **2006**, 20, 2717–2720.

(15) Ji-lu, Z. Bio-oil from fast pyrolysis of rice husk: Yields and related properties and improvement of the pyrolysis system. *J. Anal. Appl. Pyrolysis* **2007**, 80, 30–35.

(16) Chu, W.; Yang, X.; Ye, X.; Wu, Y. Vapor phase esterification catalyzed by immobilized dodecatungstosilicic acid (SiW_{12}) on activated carbon. *Appl. Catal., A* **1996**, 145, 125–140.

(17) Kirumakki, S.; Nagaraju, N.; Chary, K. Esterification of alcohols with acetic acid over zeolites, H β , HY and HZSM5. *Appl. Catal., A* **2006**, 299, 185–192.

(18) Koster, R.; van der Linden, R. B.; Poels, E.; Blik, A. The mechanism of the gas-phase esterification of acetic acid and ethanol over MCM-41. *J. Catal.* **2001**, 204, 333–338.

(19) Miao, S.; Shanks, B. Esterification of biomass pyrolysis model acids over sulfonic acid-functionalized mesoporous silicas. *Appl. Catal., A* **2009**, 359, 113–120.

(20) Gayubo, A.; Aguayo, A.; Atutxa, A.; Prieto, R.; Bilbao, J. Deactivation of a HZSM-5 zeolite catalyst in the transformation of the aqueous fraction of biomass pyrolysis oil into hydrocarbons. *Energy Fuels* **2004**, 18, 1640–1647.

(21) Milne, T. A.; Agblevor, F.; Davis, M.; Deutch, S.; Johnson, D. In *Developments in Thermal Biomass Conversion*; Bridgwater, A. V., Boock, D. G. B., Eds.; Blackie Academic and Professional: London, 1997.

(22) Simons, R. M. In *Encyclopedia of Chemical Processing and Design*; McKetta, J. J.; Cunningham, W. A., Eds.; Marcel Dekker: New York, 1983; Vol. 19, p 381.

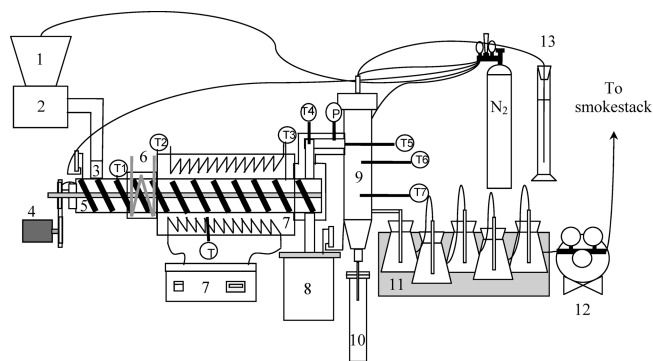


Figure 1. Continuous pyrolysis reactor including components; (1) biomass hopper, (2) vibratory feeder, (3) reactor inlet, (4) auger motor, (5) auger conveyor, (6) water cooler, (7) furnace and furnace control, (8) char collector, (9) reactive condensation unit, (10) bio-oil drip trap, (11) ice bath trap, (12) vacuum pump, and (13) ethanol container.

were subjected to pyrolysis “as received” with no preprocessing such as drying or grinding.

Bio-oil Production. Figure 1 shows the schematic of the transported-bed pyrolysis reactor used in the study. The reactor consisted of a 100 mm diameter stainless steel tube containing an auger driven by a 1/4 hp electric motor. The auger continuously transported biomass feedstock through the reactor, which was externally heated using a tube furnace (Lindberg/Blue M, model HTF55322A). The auger speed was maintained at 1.5 rpm which translated to a solid retention time of 8.3 min in the auger (residence time in the heated zone: 5.9 min).

Biomass feed was supplied to the reactor by a vibratory feeder (Eriez, model H036C). For pyrolysis experiments, the biomass feed rate was held constant to ensure consistent pyrolysis conditions. Pyrolysis vapors leaving the reactor were directed through a reactive condensation unit where ethanol was injected and then through a series of five ice-bath traps to condense any remaining bio-oil. To prevent high-boiling vapor (tar) from clogging the pyrolysis reactor and reactive condensation unit, the pyrolysis reactor’s exhaust line was heated to maintain vapor temperature above 450 °C. Slow pyrolysis conditions were assumed on the basis of the two phase-nature of the bio-oil end-product and the yield of char and gases. Noncondensable gases were removed from the system via a vacuum pump attached to the last ice-bath trap in the series and vented to atmosphere. Solids were collected in a stainless steel char collector at the outlet of the reactor, where the material was cooled at room temperature under in an inert environment. An inert atmosphere was maintained in the reactor and char collector by supplying nitrogen to various inlets in the system. The nitrogen flow rate was 3.6 L min⁻¹ distributed as follows: 2 L min⁻¹ into the main reactor, 0.5 L min⁻¹ into the hopper, 1 L min⁻¹ into the char container, and 0.1 L min⁻¹ into the reactive condensing unit. Thermocouples were installed at various locations to monitor temperatures (see Figure 1).

Reactive Condensing System. Figure 1 also shows placement of the reactor (component 9) used in the experiments to condense and esterify acidic components in the pyrolysis vapor using ethanol. The reactive condensation unit consisted of a 102 mm i.d. stainless steel tube with a reaction zone length, $L = 457$ mm, meaning the reaction zone volume was 3.8 L. In the reactor, vapors were contacted with atomized 100% (200 proof) ethanol (C₂H₅OH, abbreviated EtOH, supplied by Thermo Fisher Scientific) that was supplied using a peristaltic pump (Cole-Parmer L/S, model 7524-10) and input to the reactor by a small-bore (0.015 mm diameter) cone-spray atomizer nozzle. To achieve adequate atomization of EtOH at low flow rates (1.5–2.0 mL min⁻¹), 0.1 L min⁻¹ pressurized N₂ at 377 kPa (40 psig) was mixed with the EtOH prior to entering the

Table 1. Characterization of Solid Feedstock and Pyrolysis Char

analysis ^a	biomass	char
moisture (w.b.)	7.45	3.20
volatiles	74.83	27.58
ash	0.13	2.70
fixed carbon	17.59	69.12
C	52.60	79.1
H	5.66	3.1
N	0.18	0.2
S	0.02	0.0
O ^b	38.90	12.6
HHV (MJ/kg)	20.6	34.1

^a Measured as a percent (w/w, d.b.) unless otherwise stated.

^b By difference.

atomizer nozzle. The temperature was measured at the inlet of the reactive condensing unit and at two points along the condenser’s length. Heavier liquids condensed in a drip trap directly beneath the reactor. At a carrier gas flow rate of 3.6 L min⁻¹, the effective reactor volume (3.8 L) translated to a vapor residence time of 63.3 s in the reaction zone before entering the drip trap. Uncondensed vapor and noncondensable gases were routed through a series of five ice-bath traps that collected the remaining condensable vapor. Noncondensable gases exited to the atmosphere.

Product Yield. The quantity of biomass in the vibratory feeder hopper was weighed before and after each pyrolysis run to determine the total amount supplied to the reactor. Biomass feed rate was assumed to be steady throughout each run. Solid material, namely, char, was collected and weighed, as was condensed liquid in the drip and ice-bath traps to determine product yield. A simple mass balance was used to calculate the quantity of noncondensable gases.

For the experimental runs, the biomass feed rate was kept constant to ensure equivalent characteristics for the vapor feed entering the reactive condensing unit, while the EtOH atomization rate was varied from 0 to 6 mL min⁻¹. These runs produced samples with a WHSV from 8.3 to 33 (7.3–23.2% EtOH, w/w). The total yield of bio-oil was determined by weighing the whole product then subtracting the weight of EtOH added during the run. After total yield was determined, oily phase material from the drip and ice-bath traps was separated from aqueous phase by decanting, combined, quantified, and stored in a 4 °C refrigerator until characterized. Only oil phase material was evaluated for improvement in fuel quality. In all, five samples were generated during five one-hour pyrolysis runs. From the five samples, no less than three subsamples were taken for each characterization technique described below.

Characterization Methods. The pelletized pine feedstock used to generate bio-oil was extensively characterized prior to pyrolysis. Moisture, volatiles and ash content in the biomass and char was determined by ASTM D5142, “Standard Test Methods for Proximate Analysis of the Analysis Sample of Coal and Coke by Instrumental Procedures”, using a proximate analyzer (LECO Model TGA701). Ultimate analysis (elemental C, H, N, S, and O (by difference) in percent (w/w)) was performed in an ultimate analyzer (LECO, model CHNS-932), following ASTM D3176, “Standard Practice for Ultimate Analysis of Coal and Coke”. Table 1 shows the characterization of the pine pellet biomass (PP BM) and pine pellet char (PP CH) produced during continuous pyrolysis at 500 °C.

Bio-oils produced by the five pyrolysis runs underwent several analyses in addition to those performed on the biomass and char. Ultimate analysis was performed using a modified version of method ASTM D5291, “Standard Test Methods for Instrumental Determination of Carbon, Hydrogen, and Nitrogen in Petroleum Products and Lubricants”. In addition, water content in the oils was determined by Karl Fischer titration

using a Mettler-Toledo titrator (Model DL31), following ASTM E203, “Standard Test Method for Water Using Volumetric Karl Fischer Titration”. The higher heating value (HHV, in MJ kg⁻¹) was assessed using an isoperibol bomb calorimeter (Parr, model 1351) following ASTM D240, “Standard Test Method for Heat of Combustion of Liquid Hydrocarbon Fuels by Bomb Calorimeter”. Dynamic viscosity, η (in cP), was measured at 40 and 60 °C using a dynamic viscometer (Brookfield, model DV-I+ with UL/YZ spindle adapter) at three shear rates using a modified version of ASTM D2983, “Standard Test Method for Low-Temperature Viscosity of Lubricants Measured by Brookfield Viscometer”. Kinematic viscosity, ν (mm² s⁻¹), was determined by dividing η by density, ρ (g mL⁻¹), which was estimated using 2 mL Gay-Lussac pycnometers. The pH of the oil was measured directly using a Mettler-Toledo pH meter and probe.

We utilized a differential scanning calorimeter (DSC, Mettler-Toledo, model DSC823e) following ASTM E2009, “Standard Test Method for Oxidation Onset Temperature of Hydrocarbons by Differential Scanning Calorimetry”, to determine bio-oil stability. The oxidation onset temperature (OOT) was determined by heating a sample under an oxygen environment from 25 to 350 °C, during which time, the onset of oxidation was evidenced by a large exothermic peak. The extrapolated point formed by tangent lines extending from the baseline and from slope to the peak of oxidation was considered the OOT and higher OOTs indicate greater thermal stability. The DSC was also used to approximate the cold flow properties of the bio-oils; oils were cooled to -65 °C and then heated to 125 °C, above the melting point. Melting is indicated by an endothermic peak, and the extrapolated point where the endothermic melting peak ends is considered the cloud point. During cooling, this would be the point where crystals begin to form causing clouding. Lower cloud points indicate better cold flow properties.

The formation of esters was verified and quantified using a Hewlett-Packard (Model HP-6890) gas chromatograph containing an HP-5 MS column, 30 m in length, with a 0.25 mm i.d. and 0.25 μ m film thickness in conjunction with a Hewlett-Packard mass spectrometer (Model HP-5973) with a mass selective detector. The method used was as follows: inlet temperature of 230 °C, detector temperature at 280 °C (MS interface temperature), a flow of 1 mL min⁻¹ He, the oven initially at 40 °C for 2.5 min followed by a ramp at 8 °C min⁻¹ to 250 °C (held for 5 min). Masses were scanned from 15 to 500 mass units. The sample size was 1 μ L and was prepared for analysis by diluting to 2.5% with acetone. An internal standard, heptane, was added to each sample-acetone mixture at 0.0625% (v/v). Two model compounds in the bio-oil, acetic acid (AcOH, for acetyl hydroxide), and ethyl acetate (EA) were selected to represent an acid and an ester for quantification. Peak height ratios were calculated for AcOH and EA with the internal standard, heptane. It was assumed that some esters and acids were present in the aqueous phase. No attempts were made to quantify acids and esters in the aqueous phase material. The intent of the work was to improve only the oily phase relative to nonesterified bio-oil.

Chromatograms and spectra were viewed and compounds were identified using Agilent Technologies software (MSD ChemStation D.03.00.611), which uses a probability-based matching (PBM) algorithm to match unknown spectra to those found in a library. The mass spectral library used was the National Institute of Standards and Technology's 1998 version (NIST 98). The quality of a match determined by ChemStation is defined as the probability that the unknown is correctly identified as the reference. The quality can be between 1 and 100 with values above 90 considered very good matches.

A quantification method was developed by producing a five-point standard curve using standard solutions containing mixtures of AcOH, EA, and heptane in acetone. The standard curve

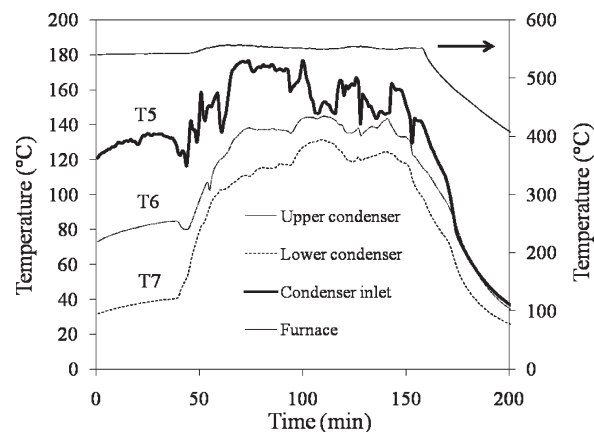


Figure 2. Cooling profile for bio-oil condensed with 7.4% EtOH (w/w) injected at 1.5 mL min⁻¹. Furnace temperature is shown on secondary vertical axis.

Table 2. Product Yield for Reactive Condensation Experiments

product	% yield (w/w) at % EtOH				
	0.0	7.3	10.3	16.4	23.2
char	21.8	23.5	23.5	24.4	24.4
gases ^a	20.6	17.8	17.0	27.2	13.9
bio-oil	57.7	58.7	59.5	48.4	61.7
oily phase					
(% of BO ^b)	17.5	21.6	17.1	19.2	9.0
(% of BM ^c)	9.0	11.6	9.6	9.5	6.0
aqueous phase					
(% of BO)	82.5	78.4	82.9	80.8	91.0
(% of BM)	42.4	42.0	36.5	40.0	40.4

^a Calculated by difference. ^b Bio-oil. ^c Biomass.

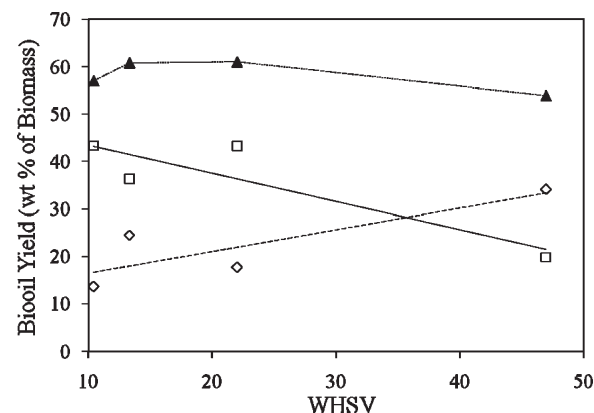


Figure 3. Relationship between WHSV and yield (wt % of original biomass) of whole oil (▲, ---), oily phase (◇, ---, $R^2 = 0.71$, p -value > 0.05) and aqueous phase (□, ---, $R^2 = 0.79$, p -value > 0.05).

yielded a least-squares best-fit line showing the concentration of AcOH and EA versus peak height ratio with heptane. This correlation was then used to predict the concentration of each of the two compounds in the bio-oil samples on the basis of the peak height ratio with heptane calculated for the bio-oils.

Results and Discussion

Bio-oil Condensing System. The condensing system effectively lowered bio-oil vapor temperature such that a liquid formed in the collector below the condenser (drip trap) prior to the ice bath traps. Figure 2 shows the temperature profile

Table 3. Characterization Data for Oily-Phase Bio-oils Produced at Various WHSV

parameter	oily phase characteristics at WHSV					
	∞	33.3	25	16.7	8.3	0
EtOH (wt %)	0	7.4	10.3	16.4	23.2	100
C	64.9 \pm 1.7 ^b	57.9 \pm 2.0	56 \pm 0.5	56.6 \pm 0.4	55.8 \pm 1.4	46.6 \pm 3.4
H	7.1 \pm 0.4	5.6 \pm 0.6	5.6 \pm 0.4	6.4 \pm 0.1	6 \pm 0.1	11.7 \pm 0.7
N	0.2 \pm 0.03	0.2 \pm 0.01	0.3 \pm 0.02	0.2 \pm 0.02	0.2 \pm 0.03	0 \pm 0.01
S	0 \pm 0.02	0 \pm 0.01	0 \pm 0.01	0 \pm 0.00	0 \pm 0.01	0 \pm 0.01
O ^a	27.8 \pm 1.4	36.3 \pm 1.9	38.1 \pm 0.5	36.7 \pm 0.4	38 \pm 1.6	41.7 \pm 0.00
HHV (MJ kg ⁻¹)	27.6 \pm 0.2	24.5 \pm 0.1	25.7 \pm 0.6	25.2 \pm 0.05	27 \pm 0.2	27.2 \pm 3.8
% H ₂ O	10 \pm 0.8	16.2 \pm 2.6	11.2 \pm 0.2	14 \pm 0.9	8.4 \pm 2.3	0.4 \pm 0.01
pH	2.48 \pm 0.01	2.65 \pm 0.02	2.74 \pm 0.03	2.82 \pm 0.02	3.05 \pm 0.01	5.29 \pm 0.4
viscosity (mm ² s ⁻¹)						
40 °C	300.1	151.2	41.3	37.2	49.2	3.75 ^c
60 °C	24.4	13.7	13.5	11.2	9.7	3.99
density (g mL ⁻¹)	1.18 \pm 0.2	1.19 \pm 0.2	1.15 \pm 0.1	1.11 \pm 0.2	1.06 \pm 0.1	0.8 \pm 0.01

^a By difference. ^b “ \pm XX.X” indicates \pm one standard deviation. ^c Ethanol viscosity as measured at 25 and 45 °C.

obtained during the run producing a bio-oil condensed with 7.4% EtOH (w/w). The start and end times for EtOH atomization during the pyrolysis run shown in Figure 2 were 60 and 150 min, respectively. The reaction zone is the region between thermocouples T6 and T7 in Figure 1, and we assume the reaction temperature to be approximately the average temperature as measured by the two thermocouples. Despite linearity, the relationship between upper condenser zone temperature and EtOH atomization rate (kg h⁻¹) was not statistically significant at $\alpha = 0.9$. The relationship between lower condenser zone temperature (°C) and EtOH atomization rate was statistically significant at $\alpha = 0.95$. These are useful observations, since condensation temperature can be controlled by EtOH and biomass feed rate to selectively condense various bio-oil components. For example, if it is desired to prevent water from condensing in the drip trap, spray volume can be adjusted such that the condenser temperature is higher than the condensing temperature of water.

Yield of Pyrolysis Products. Table 2 lists the yield of bio-oil components in percent of original biomass (w/w) and percent of total bio-oil (w/w) at each WHSV. The yield of uncondensed gas is calculated by difference such that the mass balance inevitably adds to 100%. From Figure 3, it is evident that with increasing WHSV, total oily phase yield (% of biomass, w/w) decreases while aqueous phase increases. Although it appears that with increasing WHSV the oily phase increased and the aqueous phase decreased, neither relationship was significant at $\alpha = 0.95$. However, the apparent increase in aqueous phase with concurrent decrease in water content in the oily phase relative to nonesterified bio-oil (see next section) supports the hypothesis that esterification occurred.

Pyrolysis runs with the lowest WHSV (8.3 or 26.2% EtOH (w/w)) produced a two-phase oil in the drip trap, although oily phase material condensed in the ice bath traps, as well. The aqueous phase yield in the drip trap indicated that the temperature in the reactive condensation unit was below the boiling point of some of the aqueous phase components. If desired, the temperature in the reactive condensing unit could be controlled using only EtOH to condense desired products in the drip trap.

Product Characterization. Table 3 shows characterization data for the bio-oil for each of the five pyrolysis experiments including a control run where no EtOH was added. Analysis results for untreated EtOH are also shown. Results from Table 3 indicate that the oily phase water content generally

decreases with higher EtOH atomization rate, although the relationship is not statistically significant. In addition, as evidenced by the ultimate analysis of the oils, elemental oxygen content seemed to increase with increasing EtOH. A reduction in elemental oxygen would be consistent with formation of esters assuming that no ethanol remained unreacted in the product. If carboxylic acids react with EtOH to form esters as hypothesized, the oxygen content should decrease. Theoretically, in the reaction of 1 mol of AcOH at 53.3% oxygen (w/w), with 1 mol of EtOH at 34.8% oxygen (w/w), 1 mol of ethyl acetate (EA) is formed with an oxygen content of 36.4% (w/w), which is lower than that of AcOH. Some of the oxygen from AcOH is concentrated in the reaction byproduct, water, and should partition in the aqueous phase of the condensed product and thus increase the aqueous phase yield, as seen in Figure 3 with decreasing WHSV. Since oxygen concentration does not decrease with increasing EtOH, it is likely that some ethanol remains unreacted in the bio-oil or that other reactions such as acetalizations could potentially generate higher oxygen content products.

Results indicated that as the EtOH % (w/w) was increased the water content in the oily phase decreased. Table 3 provides water content for oil collected and combined from both drip and ice bath traps. Here too, the water content decreased with increasing ethanol, although the relationship was not significant. The results are consistent with the formation of a more nonpolar bio-oil and esters. With greater ethanol volume sprayed, a greater concentration of esters in the bio-oil is expected. Since esters are less polar than the organic acids from which they are formed, water solubility in the resultant bio-oil would be expected to decline. Decreased water solubility in the bio-oil should decrease the water content in the oily phase and increase the water content in the aqueous phase.

Although lower biomass feed to ethanol spray ratios (i.e., WHSV) lowered the water content at an undetermined threshold WHSV (denoted as the single-phase threshold) between 3.8 and 8.2, the bio-oil produced existed as a single phase with high water content. This was observed during a previous experiment in which two single-phase bio-oils were generated with WHSV at 1.5 and 4.8 (57 and 28 wt % EtOH) with water content at 11.5 and 26.2 wt %, respectively. More study is needed to accurately determine the single-phase threshold. For the oily phase samples of this study, the water content was reduced by as much as 16%. Previous studies including Junming et al.¹⁰ and Zhang et al.¹⁴ witnessed

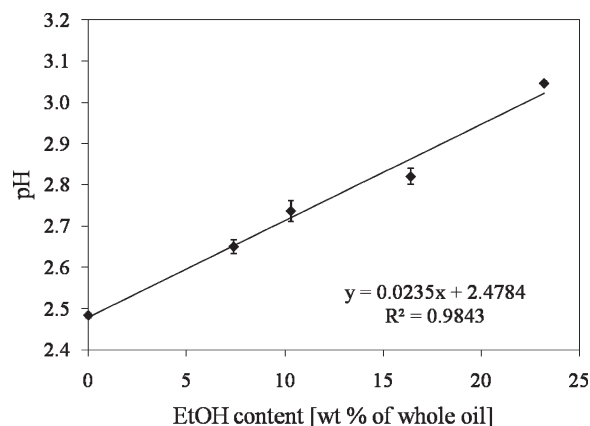


Figure 4. Relationship between pH and EtOH % (w/w).

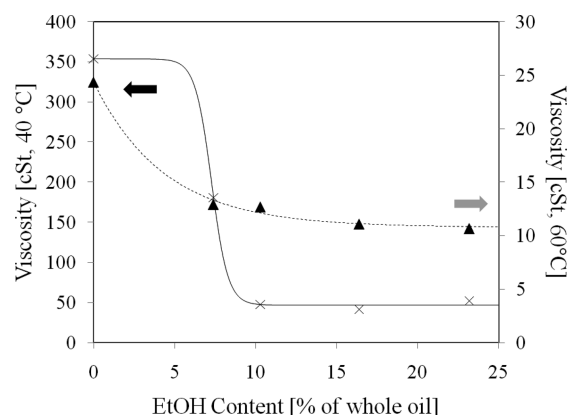


Figure 5. Viscosity at 40 °C (×, —) and at 60 °C (▲, ---) as a function of EtOH fitted with a 5-parameter sigmoidal line at $R^2 = 0.999$ and 0.996 ($p < 0.05$), respectively.

greater reductions, although their starting material, fast pyrolysis oil, has a water content at 33% compared to 10% for our control bio-oil. Nonetheless, there was no great improvement in water content achieved through reactive condensation.

Table 3 also shows high heating value (HHV in MJ kg^{-1}) for the bio-oils generated. HHV in the bio-oil increases with increasing EtOH feed rate. The sample produced at WHSV 8.3 (23.2 wt % EtOH) showed similar HHV to EtOH. Since esters, particularly ethyl acetate ($\text{HHV} = 25 \text{ MJ kg}^{-1}$), are formed in relatively high concentrations ($1.89\text{--}3.42 \mu\text{L mL}^{-1}$), it is expected that the increase in heating value is partially due to their presence. Additionally with decreasing water content, HHV should increase. For bio-oil collected from all traps, HHV ranged from 24.5 to 27.6 MJ kg^{-1} indicating little change in HHV because of esterification. Other studies¹⁴ have shown HHV increases as large as 52% (from 16 to 24 MJ kg^{-1}) when using fast pyrolysis oil as the esterification reactant. Since our starting material, slow pyrolysis bio-oil, already had a relatively high HHV at 27 MJ kg^{-1} compared to fast pyrolysis oils (16 MJ kg^{-1}) and esters ($\sim 25 \text{ MJ kg}^{-1}$), an increase caused by esterification was not clearly evident.

Another indication of the esterification reaction is the increase in pH with increasing EtOH % as shown in Figure 4. As acids such as acetic acid are consumed in the reaction with EtOH resulting in ester production, the overall acidity of the bio-oil is reduced. The relationship between pH and

Table 4. Oxidation Onset Temperature (°C) and Cloud Point Temperature (°C) for EtOH-Condensed Bio-oils

EtOH [wt %]	oxidation onset temperature [°C]		cloud point [°C]	
	av	SD	av	SD
0	174.3	1.1	−4.7	0.2
7.4	167.7	0.5	−7.3	0.4
10.3	157.1	3.1	−7.9	0.3
16.4	169.9	2.5	−6.7	1.0
23.2	172.2	1.6	−12.1	0.3

EtOH % is significant at $\alpha = 0.95$. Decreasing the acidity of bio-oil is a major goal for current research as a means to improve the fuel properties.

Another goal of bio-oil research involves lowering viscosity bio-oil such that it is similar to values specified for No. 2 diesel fuel ($1.9\text{--}4.1 \text{ mm}^2 \text{ s}^{-1}$) by ASTM D975, “Standard Specification for Diesel Fuel Oils”. Kinematic viscosity, ν , of the bio-oils is shown in Table 3. It can be seen that viscosity decreased substantially as more EtOH was added to the reactor relative to the whole oil. This is clearly evident in Figure 5 showing a nonlinear decrease in viscosity at 40 and 60 °C as a function of EtOH concentration. An interesting phenomenon to note is that although water content in the oily phase is lower at lower WHSV, which generally results in higher viscosity, we have shown the opposite to be true of the esterified oils. Using fast pyrolysis bio-oil as the reactant, Zhang et al.¹⁴ saw a decrease in viscosity from 49 to $4.9 \text{ mm}^2 \text{ s}^{-1}$ when measured at 20 °C after the bio-oil was esterified with ethanol. Our reductions were similar using slow pyrolysis bio-oil as the reactant with a reduction from 300 to as low as $37 \text{ mm}^2 \text{ s}^{-1}$ when measured at 40 °C. Moens et al.⁶ performed acid-catalyzed bio-oil esterifications while removing water by azeotropic distillation. Although they saw significant decreases in acidity (as measured by total acid number), the resulting oil was a semisolid tar with poor flow characteristics.

Table 4 shows OOT (oxidation onset temperature) and cloud point (both in °C) for the reactively condensed bio-oils. The trend for oxidation onset temperature is unclear. We expected that OOT would increase with increasing EtOH indicating an increase in stability. Other indices of stability may show improvement, but were not evaluated here. More study is needed to determine if esterification increases bio-oil stability. One measure of stability is the resistance to polymerization as evidenced by a viscosity increase. Junming et al.¹⁰ showed that after three months of aging, esterified bio-oil exhibited very little viscosity increase. Despite the lack of evidence for an increase in stability in the current study, cold flow properties were improved as evidenced by the linear decrease in cloud point as WHSV decreases (EtOH increases). A linear regression best-fit line showed an $R^2 = 0.79$ and a p -value < 0.05 . Thus, the relationship between cloud point and EtOH content is significant at $\alpha = 0.95$.

Improvements in fuel properties for esterified bio-oil as indicated by water content, HHV, pH, viscosity, and CP measurements show that progress has been made toward producing a fuel with properties more closely related to diesel fuel than unesterified bio-oil. With additional study, we will show whether esterified bio-oil can be used in diesel engines alone and in blends with diesel and biodiesel.

Figure 6 shows the chromatogram for one of the calibration samples in which the EA, AcOH, and heptane peaks are clearly evident at retention times of 1.99, 2.05, and 2.8 min, respectively. For five calibration standards, peak height

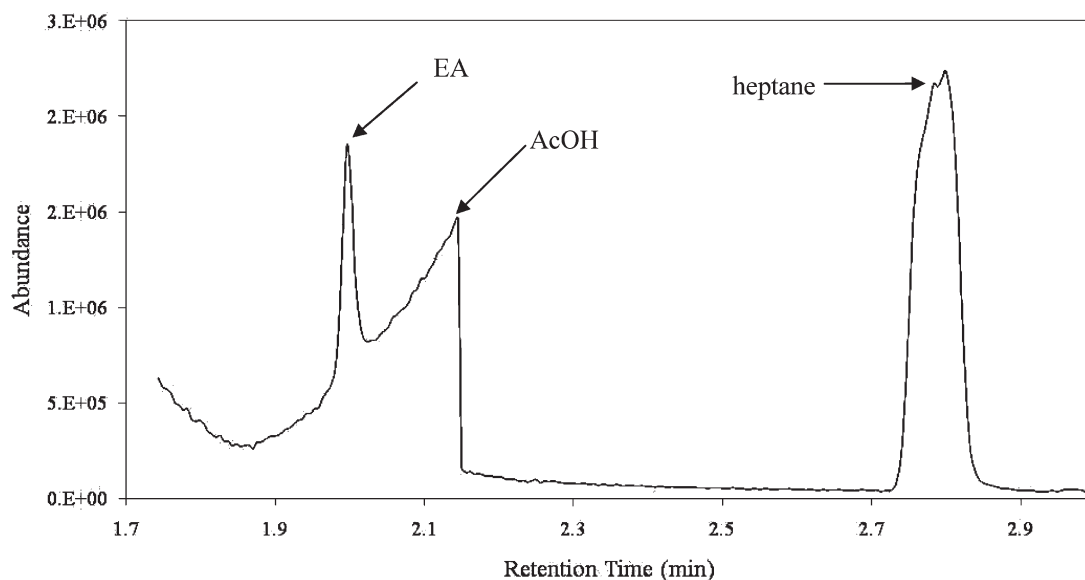


Figure 6. Gas chromatogram for calibration standard containing EA (rt = 1.999, quality = 72), AcOH (rt = 2.142, quality = 90), and heptane (rt = 2.8, quality = 90).

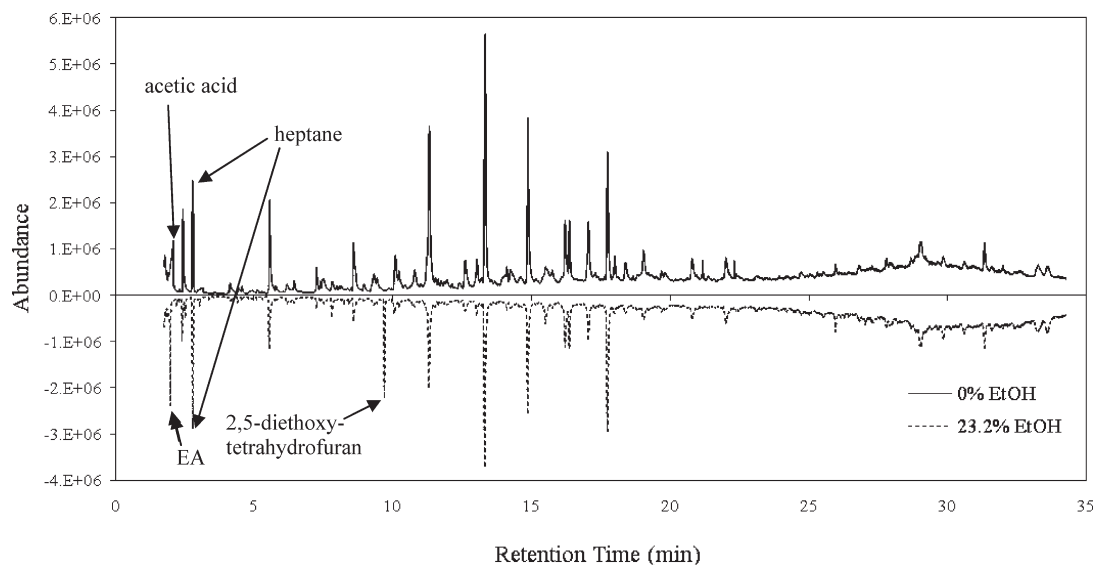


Figure 7. Bio-oil samples with 0 and 23.2% (w/w) EtOH including internal standard, heptane (rt = 2.798 min), showing EA (rt = 1.996) and AcOH (rt = 2.046) peaks.

ratios for AcOH and EtOH with heptane were determined and used to calculate concentration in experimental samples. Although ethanol likely reacts with other carboxylic acids in the bio-oil (e.g., formic, propionic, butyric acid), with aldehydes (e.g., acetaldehyde, formaldehyde, propionaldehyde, furfural) and with ketones (e.g., acetone, propanone, butanone), forming multiple products, only the effects of EtOH addition on the yield of ethyl acetate are quantified here.

Figure 7 shows the chromatograms for the control sample and for the 23.2% EtOH sample from retention times at 2–34 min. It is clear that two chromatograms are substantially similar but several key differences are clear. For one, a large peak at 9.7 min in the 23.2% sample identified as 2,5-diethoxy-tetrahydrofuran (quality = 91) does not appear in the control. This compound was likely formed as product of several reactions stemming from the interaction between EtOH and furfural, an aldehyde. Furfural is visible at

5.6 min (quality > 90) in both spectra but with lower abundance in the esterified bio-oil indicating that the concentration of furfural has been reduced. Though not quantified, acetals, products of the reaction between ethanol and aldehydes, were identified in the chromatograms. Two acetalization products were identified by the ChemStation software; in Figure 8, diethoxymethane (2.58 min) and, in Figure 9, 1,1-diethoxyethane (3.34 min) were identified in the spectrum of the 23.2% EtOH sample but not in the 0% EtOH sample. Diethoxymethane and 1,1-diethoxyethane are likely the products of EtOH with formaldehyde and acetaldehyde, respectively. However, ChemStation was not able to identify either formaldehyde or acetaldehyde in the bio-oil samples. This may be a limitation of the GC column used. An additional esterification reaction, that of propionic acid with ethanol, is indicated by the presence of propionic acid in the 0% EtOH sample but not in the 23.2% sample for which ethyl propionate, an ester, is evident.

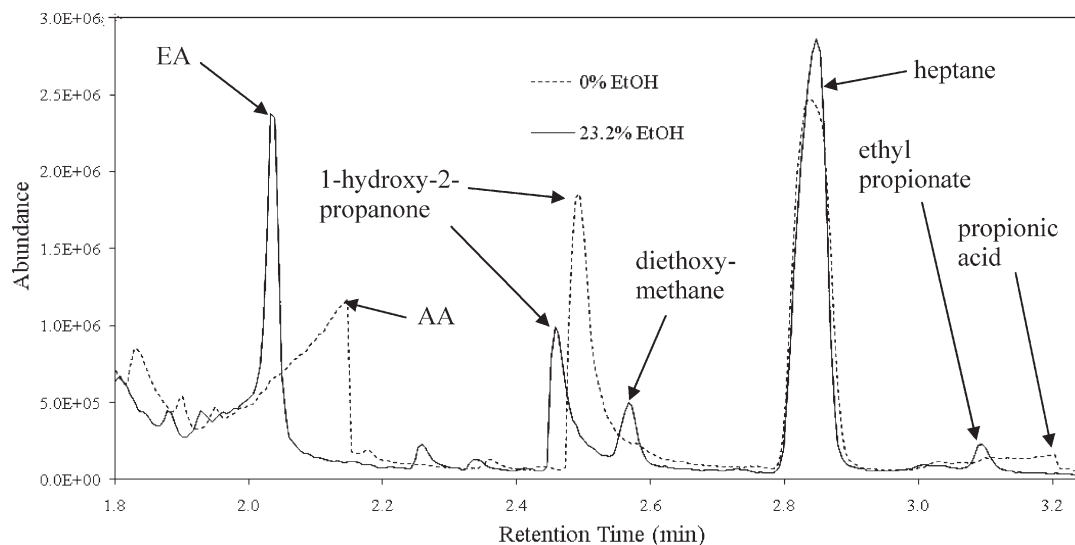


Figure 8. Gas chromatogram for 0 and 23.2% EtOH (w/w) bio-oil samples showing EA (quality = 72), AA (quality = 90), heptane (quality = 94 and 90, respectively) and various other compounds.

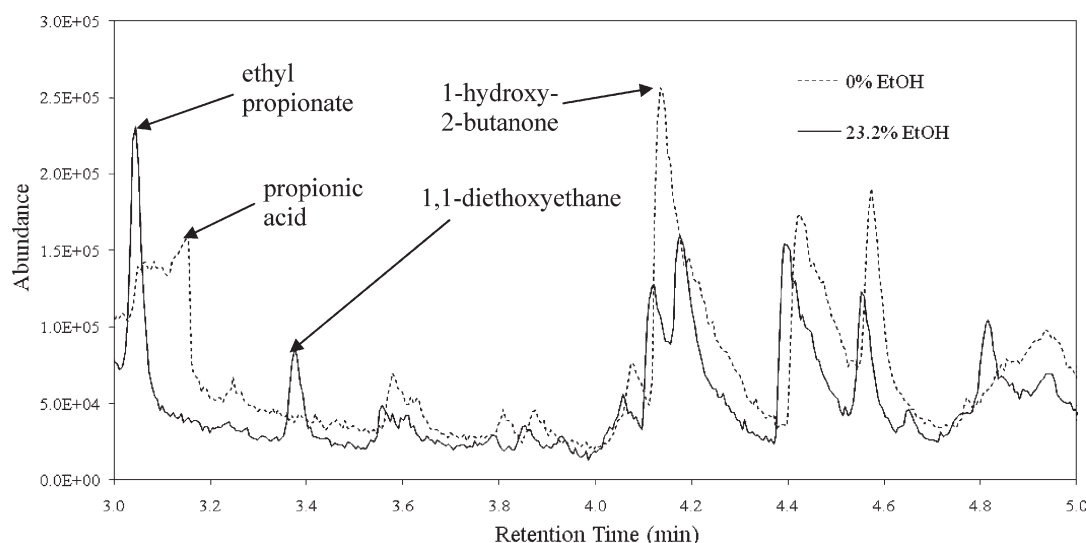


Figure 9. Chromatogram for bio-oil condensed with 0 and 23.2% (w/w) EtOH.

Figure 10 shows example chromatograms for each of the EtOH concentrations. It is clear that AA (peak B) decreases with EtOH concentration increases producing a concurrent increase in EA abundance (peak A). Peak C, 1-hydroxy-2-propanone appears to decrease relative to the internal standard indicating a reduction in concentration. Also seen in Figure 10, the small peak (F) indicating the concentration of ethyl propionate increases with increasing EtOH concentration.

The yield results from the calibrated GC-MS method are shown in Figures 11 and 12. Fractional conversion of acetic acid in % (v/v) shown in Figure 11 is calculated as the change in concentration (in mmol mL^{-1}) divided by the concentration of acetic acid (mmol mL^{-1}) in the control sample for which no ethanol was added during condensation. Both reaction temperature and EtOH concentration relative to the whole oil significantly affect (at $\alpha = 0.95$) the conversion of acetic acid. With better control of reaction zone temperature to achieve higher temperatures, it is expected that fractional conversion of acetic acid could be increased.

Figure 12 shows the fractional yield (% v/v) of ethyl acetate assuming that the expected yield is equivalent to the fractional conversion of acetic acid. The concentration of EtOH is a significant predictor of EA fractional conversion at $\alpha = 0.9$ while reaction temperature is not. It is assumed that losses of ethyl acetate during storage and transfer of bio-oil because of high volatility of ethyl acetate account for some of the variability in fractional conversion. This is likely true of other esters, as well. However, the highest yield of EA was at 23.2% EtOH and was 19%, which compares well with other studies. For example, Koster et al.¹⁸ observed EA yields that were at most 25% when using a catalyst and long reaction times (>250 min). Our method was successfully generated esters without a catalyst at reaction times of approximately 60 s.

It is clear from Figures 11 and 12 that the esterification reaction is a function of temperature and reactant concentration, since the conversion of acetic acid increased with reaction temperature (Figure 11), and as more EtOH is added, acetic acid conversion EA formation (Figure 12) increased. Ultimately, the reaction will be limited by the amount of reactants in the bio-oil vapor available for

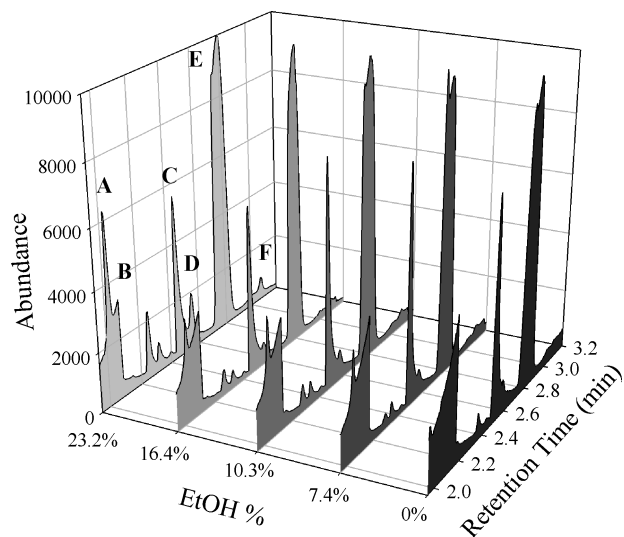


Figure 10. Stacked plot showing normalized gas chromatograms for each EtOH concentration. Compounds include EA (A), AcOH (B), 1-hydroxy-2-propanone (C), diethoxymethane (D), heptane (E), and ethyl propionate (F).

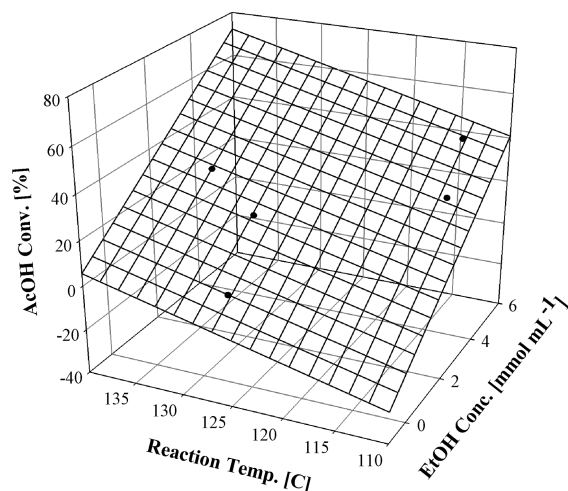


Figure 11. Fractional conversion of acetic acid (AA) as a function of reaction temperature [°C] and EtOH concentration [mmol mL⁻¹] ($R^2 = 0.996$, $p < 0.01$).

esterification. Since the reaction is reversible, it will reach equilibrium between products and reactants. The removal of water shifts the equilibrium toward products. Equilibrium for esterification reactions lie far to the right, especially if conducted in vapor phase, for which the thermodynamic equilibrium constant is 367 for the reaction of ethanol and acetic acid to form ethyl acetate.³ Because the reaction is carried out in the vapor phase, water vapor and bio-oil vapor containing reactants (e.g., acids, aldehydes, ketones) are spatially separated so water in the reaction medium affects reaction equilibria less than it would in liquid phase reactions. Thus, for the observed esterification reaction between AcOH and EtOH, the reaction strongly favors the product, ethyl acetate, with little potential for the reverse reaction between ethyl acetate and water to reform ethanol and acetic acid.

Conclusions

We have developed a method to improve the quality of bio-oil by coupling biomass pyrolysis with reactive condensation.

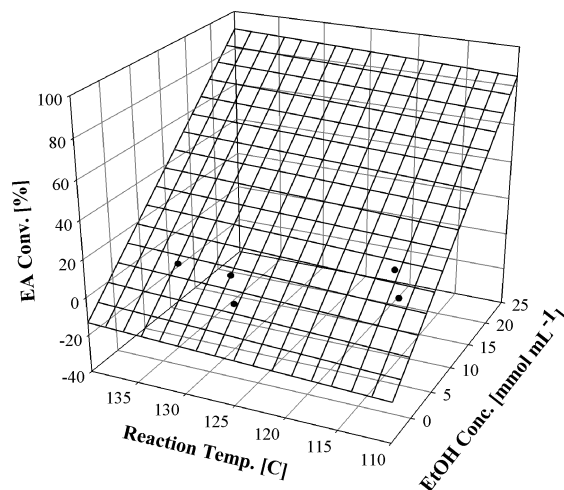


Figure 12. Fractional conversion of acetic acid to ethyl acetate (EA) as a function of reaction temperature [°C] and EtOH concentration [mmol mL⁻¹] ($R^2 = 0.89$, $p < 0.1$).

By atomizing ethanol into uncondensed bio-oil vapor produced during pyrolysis, a single integrated step, a combined condensation and esterification process has been developed. Using a reactive condensation unit, we esterified bio-oil vapor with ethanol (EtOH) at elevated temperature (114–127 °C) and reactor residence times approximating 60 s without the use of a catalyst, although any primary alcohol (e.g., methanol) could conceivably be used. GC-MS results demonstrated the formation of esters including ethyl acetate and ethyl propionate and acetals including diethoxymethane and 1,1-diethoxyethane. Quantitative GC-MS results indicated that acetic acid concentration decreased by as much as 42%, subsequently improving the pH, viscosity, and cold flow properties of the resultant bio-oil. Experiments showed the following improvements for bio-oil condensed with 23.2% EtOH (w/w) relative to the control: (i) pH was increased from 2.5 ± 0.01 to 3.1 ± 0.01 , (ii) viscosity was reduced from 24.4 to 9.7 cSt (measured at 40 °C), (iii) water content was reduced from 10 ± 0.8 to $8.4 \pm 2.3\%$ (w/w), and (iv) the cloud point was reduced from -4.7 ± 0.2 to -12.1 ± 0.4 °C.

The ability to reduce the concentration of reactive species in bio-oil is an important step in the development of stable fuel-quality pyrolysis oils derived from biomass, and esterification is one way to do so. We have shown that esterification not only reduces the concentration of a key carboxylic acid, acetic acid, it also improves overall quality of the bio-oil. Additionally, esters can be easily removed by distillation because of higher volatility compared to the acids from which they are produced. Removed esters are highly valued products in the chemical industry. When left in the bio-oil, esters improve bio-oil quality compared to the carboxylic acids they replace. It was proposed that esterified bio-oil would be more stable during aging, since acids that would normally catalyze condensation reactions leading to polymerization of bio-oil components were removed. Though not evident from the OOT results, an increase in stability may yet be observed using other stability indices such as viscosity changes during storage. The OOT value is sensitive to large variations in specific gravity: the presence of lighter, volatile compounds, such as esters, often cause materials to oxidize more readily than heavier materials.

An additional benefit to the method developed in this study is that any alcohol may be used to condense and esterify the

bio-oil vapor depending on what esters are desired as the end product. For example, if methanol, butanol or propanol is used, resulting esters will include methyl, butyl, or propyl acetate, respectively. Additionally, because of the presence of other organic acids in the oils such as formic acid, propionic acid, and butyric acid, it is possible to produce esters including formates, butyrates, and propionates in addition to the acetates observed in the current study. The relative size of the esters determines the flash point and boiling point of the bio-oil produced. A bio-oil produced by reactive condensation with methanol will have the lowest flash and boiling points. One downside to longer chain alcohols is a significant reduction in the reaction rate.²² However, if an acidic catalyst is employed, the reaction rate can be increased if required.

We expect that the esterification of bio-oil using the method described herein can be optimized for greater conversion of carboxylic acids. With better reaction zone temperature control, the reaction rate will likely induce more complete carboxylic acid conversion. In addition, this esterification method could easily be integrated into a fast pyrolysis system to improve bio-oil quality. In fact, we are currently building a fluidized-bed reactor system with an in-line esterification

reactor to test whether improvements can be made to fast pyrolysis oils. Additional studies will likely show further benefit for esterifying bio-oil, especially in further catalytic upgrading. We propose that esterified bio-oil will cause less coking on zeolite catalysts during upgrading to hydrocarbons since the cracking and deoxygenation of esters, ethyl, methyl, or otherwise, has been successfully shown in many studies.^{23–25} The removal of organic acids is beneficial because they may be precursors to coke formation on catalyst surfaces. In addition, the deoxygenation of carboxylic acids over zeolite catalysts is more difficult than esters, ketones, or aldehydes.¹¹ Esterifying organic acids prior to upgrading alleviates the difficulty by removing oxygen in the form of water since esters compared to the acids that produced them have much lower oxygen content. For example, the elemental oxygen content of acetic acid is 53.3%, while for its corresponding ester, ethyl acetate assuming ethanol was used for the esterification, the oxygen content is 36.4%. The further removal of oxygen from esters during catalytic upgrading is much easier. Thus, once catalytically upgraded, the resulting esterified bio-oil will be more like a hydrocarbon than if no esterification had been attempted.

Acknowledgment. This research was conducted through partial support from the U.S. DOE Biorefinery Research Project grants, the State of Georgia Biorefinery grant, and the UGA Experiment Station. We thank Richard Speir for carrying out pyrolysis runs and bio-oil separations. We also thank Tom Lawrence for assistance in designing the novel condensing system. Finally, we thank Joby Miller, Damion Martell, Jenille Tulloch, Kate Lee, and Elizabeth Fortner for assistance in analyzing materials.

(23) Li, H.; Shen, B.; Kabulu, J.; Nchare, M. Enhancing the production of biofuels from cottonseed oil by fixed-fluidized bed catalytic cracking. *Renewable Energy* **2009**, *34*, 1033–1039.

(24) Lima, D.; Soares, V.; Ribeiro, E.; Carvalho, D.; Cardoso, E.; Rassi, F.; Mundim, K.; Rubim, J.; Suarez, P. Diesel-like fuel obtained by pyrolysis of vegetable oils. *J. Anal. Appl. Pyrolysis* **2004**, *71*, 987–996.

(25) Ooi, Y.; Zakaria, R.; Mohamed, A.; Bhatia, S. Catalytic conversion of palm oil-based fatty acid mixture to liquid fuel. *Biomass Bioenergy* **2004**, *27*, 477–484.